Steel and Composite Structures, *Vol. 31, No. 2 (2019) 173-185*
DOI: https://doi.org/10.12989/scs.2019.31.2.173

Combined bending and web crippling of aluminum SHS members

Feng Zhou[*1,2] and Ben Young [3a]

[1] *State Key Laboratory of Disaster Reduction in Civil Engineering, Tongji University, Shanghai 200092, China*
[2] *Department of Structural Engineering, Tongji University, 1239 Siping Road, Shanghai 200092, China*
[3] *Department of Civil and Environmental Engineering, The Hong Kong Polytechnic University, Hong Kong, China*
(*Formerly, Department of Civil Engineering, The University of Hong Kong, Pokfulam Road, Hong Kong, China*)

(*Received May 10, 2018, Revised March 8, 2019, Accepted May 19, 2019*)

Abstract. This paper presents experimental and numerical investigations of aluminum tubular members subjected to combined bending and web crippling. A series of tests was performed on square hollow sections (SHS) fabricated by extrusion using 6061-T6 heat-treated aluminum alloy. Different specimen lengths were tested to obtain the interaction relationship between moment and concentrated load. The non-linear finite element models were developed and verified against the experimental results obtained in this study and test data from existing literature for aluminum tubular sections subjected to pure bending, pure web crippling, and combined bending and web crippling. Geometric and material non-linearities were included in the finite element models. The finite element models closely predicted the strengths and failure modes of the tested specimens. Hence, the models were used for an extensive parametric study of cross-section geometries, and the web slenderness values ranged from 6.0 to 86.2. The combined bending and web crippling test results and strengths predicted from the finite element analysis were compared with the design strengths obtained using the current American Specification, Australian/New Zealand Standard and European Code for aluminum structures. The findings suggest that the current specifications are either quite conservative or unconservative for aluminum square hollow sections subjected to combined bending and web crippling. Hence, a bending and web crippling interaction equation for aluminum square hollow section specimens is proposed in this paper.

Keywords: aluminum; bending; experimental investigation; finite element analysis; square hollow section; tubular sections; web crippling

1. Introduction

Aluminum alloy members are being used increasingly in architectural and structural applications. The webs of aluminum beam are prone to buckle in the absence of stiffeners at loading points (Castaldo *et al*. 2017a). If the edge load is concentrated over a portion of the element length, it is necessary to consider web crippling (Chen *et al*. 2015). Further, at the interior supports of a continuous beam or at the loading points within a span, the combined effect of bending moment and concentrated load must be considered. The combined bending moment and concentrated load could cause a reduction of capacity below that for the moment or concentrated load alone, which was obviously observed for steel members (Kövesdi *et al*. 2014, Jáger *et al*. 2015, Sundararajah *et al*. 2017).

The structural performance of aluminum beams received a lot of attention (Moen *et al*. 1999a, b, De Matteis *et al*. 2001, Piluso *et al*. 2019, Castaldo *et al*. 2017b), and a number of earlier research outcomes have already been included in major aluminum design codes (AA 2015, AS/NZS 1997, EC9 2007). The web crippling is rather complicated because it involves a number of factors, such as elastic and inelastic stability of the web element, local yielding in the immediate region of the load application, initial imperfections of plate elements and other factors (Yu 2000). Hence, the web crippling design rules in most of the specifications are empirical in nature. The web crippling and combined bending and web crippling design rules can be found in the Aluminum Design Manual (AA 2015) for aluminum structures, Australian/New Zealand Standard (1997) for aluminum structures and European Code (2007) for aluminum structures.

In the literature, there is a dearth of test results for aluminum members subjected to web crippling. Tryland *et al*. (1999) performed 52 tests on aluminum beams subjected to concentrated transverse loading that failed by web crippling. Three different sections (an I-section and two square hollow sections with different plate thicknesses) fabricated by extrusion using aluminum alloy AA6082-T6 were investigated. Zhou and Young (2008) performed 150 web crippling tests on aluminum square and rectangular hollow sections. The test specimens were fabricated by extrusion using 6063-T5 and 6061-T6 heat-treated aluminum alloys. These tests were performed under four loading conditions, namely end-one-flange (EOF), end-two-flange (ETF), interior-one-flange (IOF) and interior-two-flange (ITF) loading conditions. Zhou *et al*. (2009) also conducted 62 tests on aluminum square hollow sections subjected to concentrated loads. The tests were carried out under end (EL) and interior (IL) loading conditions, where

*Corresponding author, Associate Professor,
E-mail: zhoufeng@tongji.edu.cn
[a] Professor, E-mail: ben.young@polyu.edu.hk

ISSN: 1229-9367 (Print), 1598-6233 (Online)

the specimens were seated on a fixed solid steel base plate. These tests closely simulated the support condition of floor joist members seated on a solid foundation. The test specimens were fabricated by extrusion using 6061-T6 heat-treated aluminum alloy. The beneficial effect of the fillet corner shaping of the flange-to-web connection on the web crippling resistance for the extruded aluminum profiles was investigated by Vigh (2012). Su and Young (2018) tested 34 aluminum stocky hollow sections with web slenderness ranging from 2.8 to 28.0 subjected to concentrated transverse load, among which specimens failed by combined bending and web crippling under the IOF loading conditions. Due to relatively high CFRP to aluminum modulus ratio, it is expected that using CFRP to strengthen aluminum profiles against web crippling is an efficient method. The improved web crippling behaviour of CFRP strengthened aluminum sections was investigated by Islam and Young (2018) and Wu *et al*. (2012).

The objective of this study was to assess the appropriateness of the combined bending and web crippling design equations in the current specifications for aluminum square hollow sections. Tests were done on aluminum tubular sections subjected to combined bending and web crippling. The test specimens were extruded from a heat-treated aluminum alloy of 6061-T6. Different lengths of specimens were tested to obtain the interaction relationship between the moment and concentrated load. Furthermore, accurate finite element models (FEM) were developed for the aluminum square hollow sections subjected to each of pure bending, pure web crippling and combined bending and web crippling. The finite element analysis (FEA) program ABAQUS (2006) was used for the numerical simulation. The finite element models included geometric and material non-linearities. The interfaces between the bearing plates and the specimen were modelled carefully. The finite element models were verified against each of the pure bending tests, pure web crippling tests and combined bending and web crippling tests. A parametric study investigated the effect of cross-section geometries on the combined bending and web crippling strengths of aluminum square hollow sections. The combined bending and web crippling test results, as well as the strengths predicted from the FEA, were compared with the design strengths obtained using the American (AA 2015), Australian/New Zealand (AS/NZS 1997) and European (EC9 2007) specifications for aluminum structures. A bending and web crippling interaction equation for aluminum square hollow sections is proposed in this paper as a consequence of the study findings.

The pure bending test results reported by Zhu and Young (2009) and the pure web crippling test results for IL loading condition reported by Zhou *et al*. (2009) have been used in this paper. The pure bending test results and the pure web crippling test results are needed to nondimensionalize the combined bending and web crippling tests as described in this paper. The results of the pure web crippling tests are also compared with the design strengths obtained using the AA Specification, AS/NZS Standard and EC9 Code for reference only. The focus of this paper is the investigation of the aluminum tubular members subjected to combined bending and web crippling.

2. Experimental investigation

2.1 Pure bending tests (*Zhu and Young 2009*)

Zhu and Young (2009) reported the tests of aluminum alloy square hollow sections (SHS) subjected to pure bending, which were used to nondimensionalize the combined bending and web crippling tests as described in this paper. The beam specimens were extruded from a heat-treated aluminum alloy of 6061-T6 and belonged to the same batch of specimens as the combined bending and web crippling tests. The material properties of the specimens related to the combined bending and web crippling tests are summarized in Table 1. The material properties of the specimens presented in Table 1 were obtained from tensile coupon tests. The tensile coupons were taken from the center of the web plate in the longitudinal direction of the untested specimens. The tensile coupon dimensions conformed to the Australian Standard AS 1391 (1991) and the ASTM Standard (1997) for the tensile testing of metals, using a 12.5 mm wide coupon and a gauge length of 50 mm. Table 1 includes measured initial Young's modulus (E), static 0.2% tensile proof stress ($s_{0.2}$), static tensile strength (s_u) and elongation after fracture (e_f) based on a gauge length of 50 mm. The details of the pure bending tests have been described by Zhu and Young (2009).

2.2 Pure web crippling tests (*Zhou et al*. *2009*)

Zhou *et al*. (2009) reported a test program on aluminum alloy tubular sections subjected to concentrated bearing loads. The test specimens consisted of square hollow sections that belonged to the same batch of specimens as the combined bending and web crippling tests. The material properties obtained from the tensile coupon tests are shown, therefore, in Table 1. The tests were carried out under the two loading conditions of end loading (EL) and interior loading (IL). The specimens were loaded using different bearing lengths *N* and the flanges of the specimens were not fastened (unrestrained) to the bearing plates.

Earlier research by Zhao and Hancock (1992) on tubular sections subjected to interior loading, and combined bending and web crippling, has shown that design models for bearing are based on two different types of failure. These are web buckling, where the web of the section under compression is analyzed as a column, and web yielding, where the web and flange participate in a plastic collapse mechanism. Both modes of failure need to be checked as

Table 1 Material properties obtained from tensile coupon tests (Zhu and Young 2009)

Section (d×b×t)	E (GPa)	$\sigma_{0.2}$ (MPa)	σ_u (MPa)	ε_f (%)
32×32×2	66.4	242.9	260.6	9.9
50×50×3	63.6	268.1	273.4	10.2
76×76×3	68.1	245.5	263.8	9.5
100×100×2.3	67.9	233.9	257.7	9.6

Table 2 Comparison of pure web crippling test strengths with design strengths for interior loading condition

Specimen	Bearing length	Exp. ult. load per web	Design		Comparison	
	N (mm)	P_{Exp} (kN)	P_{AA} & $P_{AS/NZS}$ (kN)	P_{EC9} (kN)	$\frac{P_{Exp}}{P_{AA}}$ & $\frac{P_{Exp}}{P_{AS/NZS}}$	$\frac{P_{Exp}}{P_{EC9}}$
W-32×32×2N30	30	22.4	12.4	24.0	1.81	0.93
W-50×50×3N30	30	37.0	32.2	49.4	1.15	0.75
W-50×50×3N60	60	47.9	38.0	64.2	1.26	0.75
W-76×76×3N30	30	34.5	31.4	45.9	1.10	0.75
W-76×76×3N60	60	48.7	36.6	54.2	1.33	0.90
W-100×100×2.3N60	60	29.3	19.9	25.6	1.48	1.15
W-100×100×2.3N90	90	30.2	23.0	29.3	1.31	1.03
Mean					1.35	0.89
COV					0.177	0.175

part of a design. Hence, the pure web crippling test strengths obtained from the study by Zhou *et al*. (2009) were compared with the nominal strengths (unfactored design strengths) obtained using the AS 4100 (1998) and BS 5950 Part 1 (2000). It was shown that the design equations of web bearing yield in the AS 4100 do not predict well the web bearing yield strength for the aluminum square hollow sections with sharp corners, and the design strengths predicted by the BS 5950 Part 1 are generally unconservative. Hence, the modified web crippling design equations have been proposed, based on the test results. The pure web crippling tests and the modified web crippling design equations were detailed by Zhou *et al*. (2009).

The values of the experimental ultimate web crippling load per web (P_{Exp}) and the nominal web crippling strength of the IL loading condition predicated using the AA Specification, AS/NZS Standard and EC9 Code for aluminum structures are given in Table 2. These values are needed to nondimensionalize the combined bending and web crippling tests as described in this paper. The values of the nominal web crippling strength shown in Table 2 were calculated using the material properties obtained from the longitudinal tension coupon tests. The AS/NZS Standard has adopted the web crippling design rules from the AA Specification, and no changes have been introduced into the web crippling design rules. Hence, the web crippling design strengths predicted by the AA Specification and the AS/NZS Standard are identical. The test strengths were compared with the unfactored design strengths obtained using the AA Specification, AS/NZS Standard and EC9 Code for aluminum structures, as shown in Table 2. It can be concluded that the AA Specification and AS/NZS Standard are conservative while the EC9 Code is generally unconservative. The mean value of the tested-to-predicted web crippling ratios P_{Exp}/P_{AA} and $P_{Exp}/P_{AS/NZS}$ was 1.35 with the corresponding COV of 0.177 while P_{Exp}/P_{EC9} was 0.89 with the corresponding COV of 0.175.

2.3 Combined bending and web crippling tests

The combined bending and web crippling tests were conducted on the same batch of specimens as the pure bending and pure web crippling tests for the 6061-T6 heat-treated aluminum alloy. Hence, the material properties of the test specimens were identical to those shown in Table 1. Four square hollow sections (32×32×2, 50×50×3, 76×76×3 and 100×100×2.3) were tested. The test specimens had the nominal overall depth of the webs (d) and nominal flange widths (b) ranging from 32 to 100 mm, and nominal thicknesses (t) ranging from 2.0 to 3.0 mm. The measured web slenderness (h / t) values ranged from 14.3 to 42.2. Table 3 shows the measured test specimen dimensions using the nomenclature defined in Fig. 1. The specimen length (L) was varied in order to determine the interaction relationship between moment and concentrated load. The length of the specimens was calculated based on the factor a determined as follows

$$a = \frac{kM_{Exp}}{P_{Exp}} \tag{1}$$

Eq. (1) was suggested by Zhao and Hancock (1992) for the square and rectangular hollow sections. In Eq. (1), a is the distance from the centre of the loading point to the support point, as shown in Fig. 2, M_{Exp} is the experimental ultimate moment obtained from the pure bending tests of

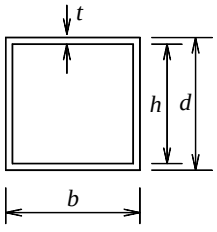

Fig. 1 Definition of symbols

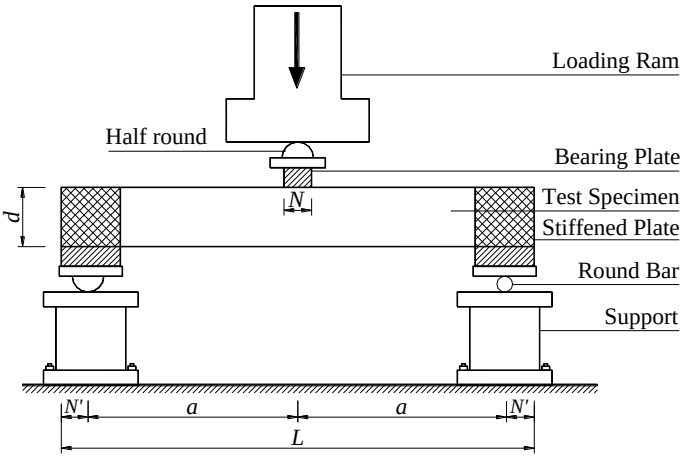

(a) Front view

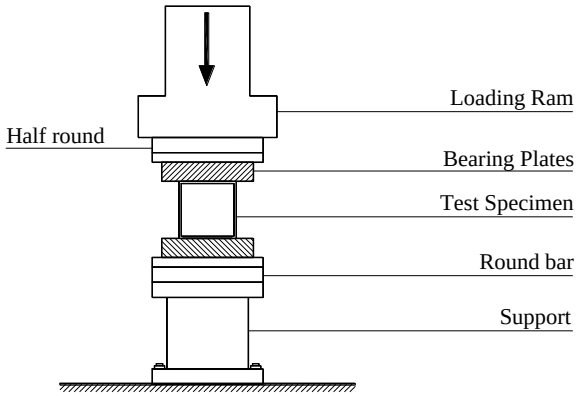

(b) End view

Fig. 2 Schematic views of combined bending and web crippling test arrangement

the same size of section, P_{Exp} is the experimental ultimate load per web obtained from the pure web crippling tests under IL loading condition of the same size of section with different bearing lengths, and k is the interaction factor that determines the interaction relationship between moment and concentrated load. Generally, the k factor was chosen at 0.7, 1.3 and 2.0 for all sections. Tests with lower values of k result in lower ratios of moment to concentrated load, whereas tests with higher values of k result in higher ratios of moment to concentrated load. The concentrated load was applied by means of bearing plates, which acted across the full flange widths of the hollow sections. The bearing plates were fabricated using quench and tempered high strength steel having a nominal yield stress of 800 MPa with a plate thickness of 50 mm. The flanges of the hollow section specimens were not fastened (unrestrained) to the bearing plates during testing.

In Table 3, the specimens were labelled such that the test type, the nominal dimension of the specimen, bearing length and interaction factor could be identified from the label. For example, the label "C-50×50×3N30K0.7" defines the combined bending and web crippling test specimen with nominal cross-section dimension ($d \times b \times t$) of 32 × 32 × 2 mm, where the notation "N30" indicates the bearing length in mm (30 mm) and the notation "K1.5" indicates the interaction factor of 0.7.

The schematic views of the combined bending and web crippling test arrangement are shown in Figs. 2(a) and (b) for the front and end views, respectively. Different lengths of specimens were tested. A bearing plate was positioned at the mid-length of the specimen. The specimen was supported on two steel plates at both ends of it. Stiffened plates were used at the ends of the specimen to prevent web crippling caused by the concentrated reaction load. Hinge and roller supports were simulated by half round and round bars, respectively. Photographs of the combined bending and web crippling test setup are shown in Fig. 3(a).

The same testing machine was used in the combined bending and web crippling tests as the pure web crippling tests. A DARTEC servo-controlled hydraulic testing machine was used to apply a concentrated compressive force to the test specimens. Displacement control was used to drive the hydraulic actuator at a constant speed of 0.3 mm/min for all test specimens. A TML data acquisition system was used to record the load at regular intervals during the tests.

The experimental results of the combined bending and web crippling tests are given in Table 3. The experimental ultimate loads per web ($P_{C\text{-}Exp}$) obtained from the tests were used to calculate the experimental ultimate moments of the sections ($M_{C\text{-}Exp}$). The moments were calculated using one-half of the ultimate applied load from the actuator multiplied by the distance from the centre of the loading point to the centre of the support point of the specimens.

Table 3 Measured specimen dimensions and experimental results of combined bending and web crippling tests

Specimen	Web	Flange	Thickness	Length	Experimental ultimate load per web	Experimental ultimate moment
	d	*b*	*t*	*L*	$P_{C\text{-}Exp}$	$M_{C\text{-}Exp}$
	(mm)	(mm)	(mm)	(mm)	(kN)	(kN.m)
C-32×32×2N30K1.3	31.86	31.92	1.947	110	20.5	0.82
C-32×32×2N30K2.0	31.90	31.88	1.949	152	14.9	0.91
C-50×50×3N30K0.7	50.35	50.92	3.085	137	36.5	1.93
C-50×50×3N30K1.3	50.39	50.70	3.079	228	26.8	2.65
C-50×50×3N30K2.0	50.41	50.72	3.084	335	19.5	2.98
C-50×50×3N60K1.3	50.39	50.72	3.082	213	43.9	3.38
C-50×50×3N60K2.0	50.74	50.42	3.044	295	31.0	3.66
C-76×76×3N30K0.7	75.93	75.92	3.037	261	30.8	3.54
C-76×76×3N30K1.3	75.92	75.93	3.066	456	24.8	5.27
C-76×76×3N30K2.0	75.94	75.95	3.062	685	16.1	5.28
C-76×76×3N60K0.7	76.04	76.05	3.082	224	53.5	4.33
C-76×76×3N60K1.3	76.07	76.01	3.080	362	43.5	6.57
C-76×76×3N60K2.0	76.02	76.01	3.071	525	28.8	6.67
C-102×102×2.3N60K0.7	101.64	101.79	2.309	355	31.8	4.70
C-102×102×2.3N60K1.3	101.62	101.85	2.310	609	23.8	6.51
C-102×102×2.3N60K2.0	101.64	101.85	2.306	904	16.8	7.07
C-102×102×2.3N90K0.7	101.80	101.67	2.301	348	38.5	5.54
C-102×102×2.3N90K1.3	101.64	101.78	2.302	594	26.5	7.08
C-102×102×2.3N90K2.0	101.79	101.65	2.301	882	17.5	7.19

Out-of-plane bending of the specimens was not observed in the tests.

3. Finite element analysis

The finite element program ABAQUS (2006) was used to simulate aluminum tubular sections subjected to pure bending, pure web crippling and combined bending and web crippling. The components of bearing plates, aluminum tubular section and the interfaces between the bearing plates and the aluminum section have been considered carefully in the finite element models (FEM).

In the FEM, the measured cross-section dimensions and material properties obtained from the tests were used. The models were based on the centreline dimensions of the cross-sections. The bearing plates were modelled using analytical rigid plates and the aluminum sections were modelled using the S4R shell elements. The S4R element is a four-node doubly curved thin or thick shell element with reduced integration, hourglass control and finite membrane strains. It is mentioned in the ABAQUS manual that S4R element is suitable for complex buckling behaviour. The S4R element has six degrees of freedom per node and

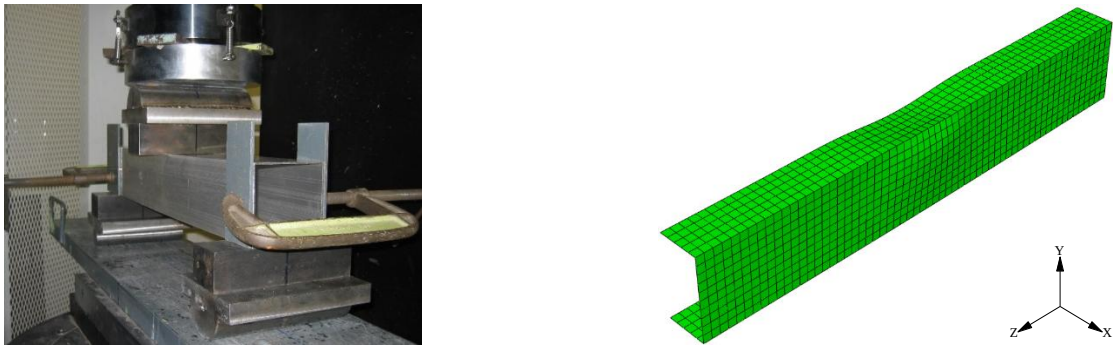

(a) Experimental (b) FEA

Fig. 3 Comparison of experimental and finite element analysis failure mode for combined bending and web crippling tests

provides accurate solutions to most applications (2006). The finite element mesh used in the model was investigated by varying the size of the elements in the cross-section to provide both accurate results and less computational time. The finite element mesh sizes ranging from 2×2 mm (length by width) to 10×10 mm were used for the flanges and webs depending on the size of the sections. The typical finite element mesh of the square hollow section is shown in Fig. 3(b).

The interfaces between the bearing plates and the aluminum section were modelled using the contact pair. The steel bearing plates are the master elements, while the aluminum specimen is the slave element of the interface elements in the finite element model. The coefficient of friction between the contacting surfaces was taken as 0.3 in the analysis. The contact pair allowed the surfaces to separate under the influence of a tensile force. However, the two contact surfaces were not allowed to penetrate each other.

Following the test procedure, the boundary conditions were modelled carefully and accurately for pure bending tests, pure web crippling tests and combined bending and web crippling tests, respectively. Due to symmetry, only one half of the specimen was modelled, as shown in Fig. 3(b). The nodes of the symmetry of the section were prevented from translational displacement in the X direction and rotation about the Y and Z axes.

The loading method used in the finite element analysis (FEA) was identical to that used in the tests. The displacement control method was used for the analysis of the aluminum section subjected to pure bending, pure web crippling and combined bending and web crippling. The transverse compressive load was applied to the specimen by specifying a displacement to the reference point of the analytical rigid plate that modelled the bearing plate. Generally, a displacement of 100 mm, 10 mm and 50 mm was specified for pure bending tests, pure web crippling tests and combined bending and web crippling tests, respectively.

The measured stress-strain curves of the specimens were used in the FEA. The material behaviour provided by ABAQUS allows for the multi-linear stress-strain curve to be used. The first part of the multi-linear curve represents the elastic part up to the proportional limit stress with measured Young's modulus as well as the Poisson's ratio of 0.33. Since the analysis of post buckling involves large in-elastic strains, the nominal (engineering) static stress-strain curve was converted to a true stress and logarithmic plastic strain curve. The equations for the true stress (s_{true}) and plastic true strain $\left(\varepsilon_{true}^{pl}\right)$ were specified in ABAQUS (2006).

The overall and local geometrical imperfections have negligible effects on web crippling behaviour, especially for hollow sections (Gardner and Nethercot 2004, Zhou and Young 2007, 2010), hence were not included in the FEM for both pure web crippling and combined bending and web crippling specimens. For pure bending specimens, only local geometric imperfections were incorporated in the FEM in the form of the lowest buckling mode shape predicted from the linear perturbation analysis. The magnitude of the imperfections was considered as 0.02*t*, where *t* is the thickness of the specimens. For all pure bending, pure web crippling, and combined bending and web crippling specimens, residual stresses were not included in the model. This is because extruded aluminum alloy profiles have small residual stresses, and for practical purpose these small values of residual stresses have a negligible effect on load-bearing capacity (Mazzolani 1995).

4. Verification of finite element models

In the verification of the FEM, 4, 7 and 16 aluminum tubular specimens subjected to pure bending, pure web crippling and combined bending and web crippling were analyzed, respectively. A comparison was carried out between the experimental results and the finite element results. The main objective of this comparison was to verify and check the accuracy of the finite element models. The comparison of the test results with the numerical results is shown in Tables 4, 5 and 6 for the pure bending tests, pure web crippling tests and combined bending and web crippling tests, respectively. It can be seen that very good agreement was achieved between the experimental and the corresponding coefficients of variation of 0.067, 0.040

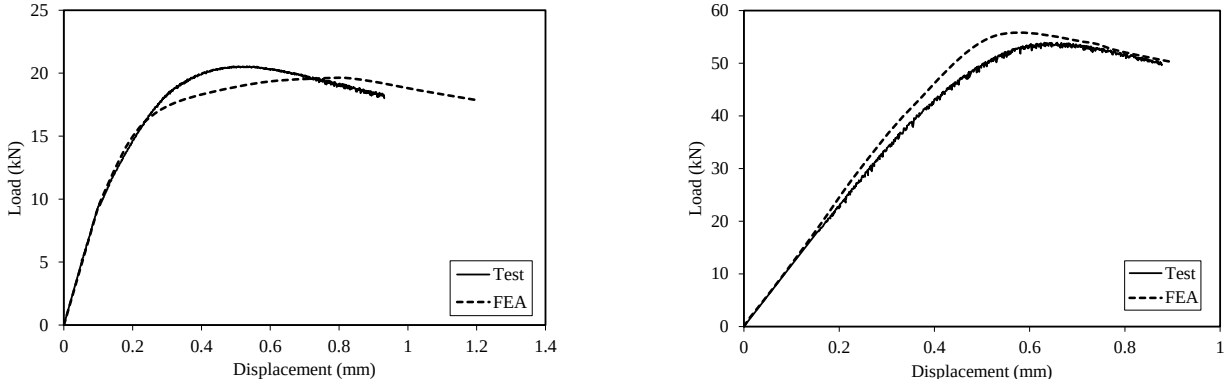

(a) Specimen C-32×32×2N30K1.3 (b) Specimen C-76×76×3N60K0.7

Fig. 4 Typical comparison of experimental and numerical load-displacement curves for combined bending and web crippling specimens

Table 4 Comparison of experimental results with pure bending strengths predicted from finite element analysis

Specimen	Web slenderness	Exp. moment	FEA moment	Comparison
	h/t	M_{Exp} (kN.m)	M_{FEA}(kN.m)	M_{Exp}/M_{FEA}
B-32×32×2	14.5	0.68	0.69	0.99
B-50×50×3	14.3	2.82	2.60	1.08
B-76×76×3	22.5	5.65	6.00	0.94
B-100×100×2.3	42.2	6.19	6.56	0.94
			Mean	0.99
			COV	0.067

Table 5 Comparison of experimental results with pure web crippling strengths predicted from finite element analysis

Specimen	Web slenderness	Exp. load per web	FEA load per web	Comparison
	h/t	P_{Exp} (kN.m)	P_{FEA} (kN.m)	P_{Exp}/P_{FEA}
W-32×32×2N30	14.4	22.4	21.5	1.04
W-50×50×3N30	14.7	37.0	39.0	0.95
W-50×50×3N60	14.7	47.9	51.8	0.92
W-76×76×3N30	22.7	34.5	35.9	0.96
W-76×76×3N60	22.8	48.7	51.8	0.94
W-100×100×2.3N60	42.2	29.3	29.6	0.99
W-100×100×2.3N90	41.8	30.2	31.2	0.97
			Mean	0.97
			COV	0.040

Table 6 Comparison of experimental results with combined bending and web crippling strengths predicted from finite element analysis

Specimen	Web slenderness	Experimental ultimate load per web	FEA ultimate load per web	Comparison
	h/t	P_{Exp} (kN.m)	P_{FEA} (kN.m)	P_{Exp}/P_{FEA}
C-32×32×2N30K1.3	14.4	20.5	19.6	1.05
C-32×32×2N30K2.0	14.4	14.9	15.1	0.98
C-50×50×3N30K0.7	14.3	36.5	35.2	1.04
C-50×50×3N30K1.3	14.4	26.8	29.7	0.90
C-50×50×3N30K2.0	14.3	19.5	20.3	0.96
C-50×50×3N60K1.3	14.3	43.9	45.2	0.97
C-50×50×3N60K2.0	14.7	31.0	31.0	1.00
C-76×76×3N60K0.7	22.7	53.5	55.0	0.97
C-76×76×3N60K1.3	22.7	43.5	48.0	0.91
C-76×76×3N60K2.0	22.8	28.8	31.9	0.90
C-102×102×2.3N60K0.7	42.0	31.8	30.4	1.04
C-102×102×2.3N60K1.3	42.0	23.8	24.1	0.99
C-102×102×2.3N60K2.0	42.1	16.8	16.6	1.01
C-102×102×2.3N90K0.7	42.2	38.5	36.0	1.07
C-102×102×2.3N90K1.3	42.2	26.5	27.9	0.95
C-102×102×2.3N90K2.0	42.2	17.5	17.9	0.98
			Mean	0.98
			COV	0.053

Table 7 Pure bending, pure web crippling and combined bending and web crippling strengths predicted from finite element analysis of parametric study

Section	Slend.	Pure bending	Pure web crippling	Combined bending and web crippling					
		FEA ultimate moment	FEA ultimate load per web	FEA ultimate load per web and FEA ultimate moment					
				K = 0.7		K = 1.3		K = 2.0	
	h/t	M_{FEA}	P_{FEA}	$P_{C\text{-}FEA}$	$M_{C\text{-}FEA}$	$P_{C\text{-}FEA}$	$M_{C\text{-}FEA}$	$P_{C\text{-}FEA}$	$M_{C\text{-}FEA}$
	(mm)	(kN.m)	(kN)	(kN)	(kN.m)	(kN)	(kN.m)	(kN)	(kN.m)
150×150×1.7N75	86.2	8.2	13.3	13.0	5.6	8.3	6.6	6.0	7.4
150×150×1.7N150	86.2	8.2	15.1	17.4	6.6	11.9	8.4	7.8	8.5
150×150×2.5N75	58.0	14.2	33.1	32.9	9.9	24.3	13.5	16.4	14.0
150×150×2.5N150	58.0	14.2	38.4	45.4	11.7	31.9	15.3	21.3	15.7
150×150×3.0N75	48.0	18.6	47.8	51.7	14.1	36.5	18.5	24.2	18.9
150×150×3.0N150	48.0	18.6	56.7	69.1	15.9	50.0	21.4	35.1	23.1
150×150×3.5N75	40.9	24.1	67.0	71.8	18.1	50.4	23.5	33.5	24.1
150×150×3.5N150	40.9	24.1	78.8	96.5	20.6	70.4	28.0	46.0	28.1
150×150×4.5N75	31.3	35.9	100.9	117.5	29.2	74.5	34.4	48.9	34.8
150×150×4.5N150	31.3	35.9	141.0	171.1	30.5	114.5	37.9	77.3	39.3
150×150×12.0N75	10.5	112.8	516.0	539.1	82.5	372.5	105.9	243.0	106.3
150×150×12.0N150	10.5	112.8	721.2	…	…	620.5	126.2	406.6	127.2
200×200×2.0N100	98.0	17.1	16.6	17.4	12.6	10.2	13.7	8.0	16.5
200×200×2.0N200	98.0	17.1	19.0	21.8	13.8	14.4	16.9	9.4	17.0
200×200×2.5N100	78.0	22.9	30.7	36.2	18.9	23.9	23.1	15.8	23.5
200×200×2.5N200	78.0	22.9	38.1	40.4	17.0	29.6	23.1	19.6	23.5
200×200×3.0N100	64.7	29.2	47.1	48.9	21.2	33.3	26.9	22.8	28.3
200×200×3.0N200	64.7	29.2	54.0	62.4	23.6	49.5	34.8	32.6	35.3
200×200×5.5N100	34.4	70.9	163.2	167.2	50.9	129.3	73.0	84.6	73.5
200×200×5.5N200	34.4	70.9	201.8	255.0	62.7	161.7	73.9	116.6	81.9
200×200×9.0N100	20.2	129.7	377.2	421.6	101.5	291.9	130.5	202.3	139.1
200×200×9.0N200	20.2	129.7	551.1	…	…	501.9	153.6	344.8	162.3
200×200×25.0N100	6.0	403.2	1822.7	1914.2	296.4	1330.3	382.6	875.0	387.1
200×200×25.0N200	6.0	403.2	2445.9	…	…	2263.5	485.1	1486.8	490.2

numerical results for all specimens. The mean values of the M_{Exp}/M_{FEA} or P_{Exp}/P_{FEA} ratio are 0.99, 0.97 and 0.98 with and 0.053 for pure bending tests, pure web crippling tests and combined bending and web crippling tests, respectively. A maximum difference of 10% was observed between the experimental and numerical results for specimens C-50×50×3N30K1.3, C-50×50×3N60K2.0 and C-76×76×3N60K2.0. The failure mode observed from the tests was also verified by the finite element model. The comparison of failure modes between experimental and numerical results for aluminum specimens subjected to combined bending and web crippling is shown in Fig. 3. Typical comparison of experimental and numerical load-displacement curves for Specimens C-32×32×2N30K1.3 and C-76×76×3N60K0.7 are shown in Fig. 4, indicating that the FEM is able to replicate the initial stiffness and the general shape of the experimental curves accurately. Good agreement was found between the experimental and finite element results for web crippling strengths, failure modes and load-displacement curves.

5. Parametric study

It was found that the FEM closely predicted the behaviour of aluminum square hollow sections subjected to pure bending, pure web crippling and combined bending and web crippling. Hence, a parametric study was carried out to study the effect of cross-section geometries on the strengths of aluminum square hollow sections subjected to combined bending and web crippling. A total of 117 specimens was analyzed in the parametric study and the cross-section dimensions and strengths (M_{FEA}, P_{FEA}, $P_{C\text{-}FEA}$ and $M_{C\text{-}FEA}$) predicted from the FEA are summarized in Table 7. The specimens consisted of sixteen different section sizes, having the overall web depths (d) of 150 and 200 mm and the thicknesses (t) ranging from 1.7 to 25.0 mm. The web slenderness (h / t) value ranged from 6.0 to 86.2. The measured stress-strain curve of the flat portion of section 76×76×3 was used in the parametric study.

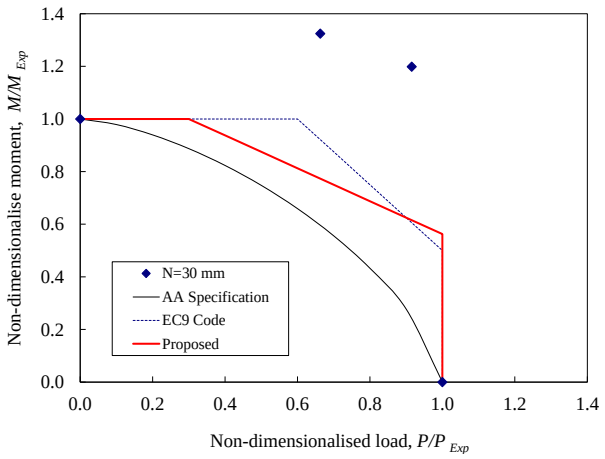

Fig. 5 Comparison of combined bending and web crippling test strengths with design strengths for square hollow section 32×32×2

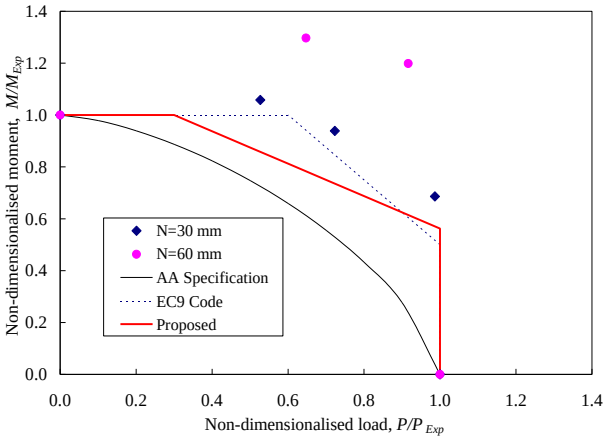

Fig. 6 Comparison of combined bending and web crippling test strengths with design strengths for square hollow section 50×50×3

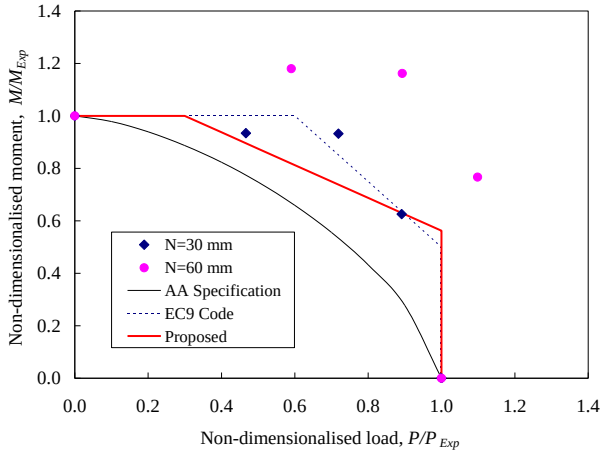

Fig. 7 Comparison of combined bending and web crippling test strengths with design strengths for square hollow section 76×76×3

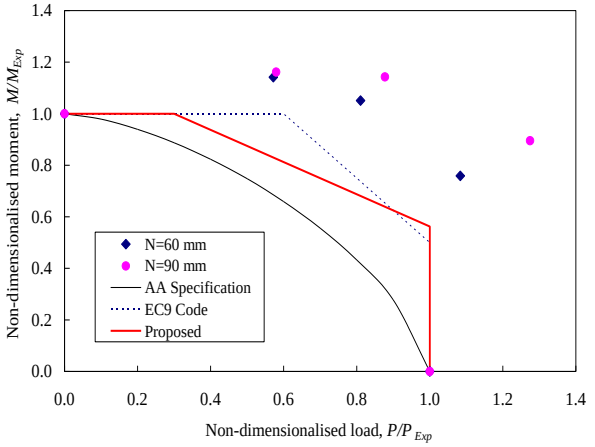

Fig. 8 Comparison of combined bending and web crippling test strengths with design strengths for square hollow section 102×102×2.3

6. Comparison of experimental and numerical results with current design strengths

The experimental results obtained from the combined bending and web crippling tests and numerical strengths predicted from the finite element analysis were compared with the nominal strengths (unfactored design strengths) predicted using the AA Specification (2015), AS/NZS Standard (1997) and EC9 Code (2007) for aluminum structures. The AS/NZS Standard has adopted the combined bending and web crippling design rules from the AA Specification, and no changes have been introduced in these design rules. Therefore, the design strengths predicted by the AA Specification and AS/NZS Standard are identical. In the AA Specification and AS/NZS Standard, the nominal strengths are calculated using the following interaction equation

$$\left(\frac{P}{P_{Exp}}\right)^{1.5}+\left(\frac{M}{M_{Exp}}\right)^{1.5}\le 1.0 \tag{2}$$

where P is the required web crippling strength per web, P_{Exp} is the experimental web crippling load per web obtained from the pure web crippling tests, M is the required flexural strength of the sections and M_{Exp} is the experimental ultimate moment of the sections obtained from the pure bending tests.

In the EC9 Code, the nominal strengths are calculated using the following interaction equation

$$\left(\frac{P}{P_{Exp}}\right)+0.8\left(\frac{M}{M_{Exp}}\right)\le 1.4 \tag{3}$$

A comparison of the combined bending ($M_{\text{C-Exp}}$) and web crippling ($P_{\text{C-Exp}}$) test strengths with the design strengths obtained from Eqs. (2) and (3) for aluminum square hollow sections are shown in Figs. 5-20. The horizontal axis of these figures shows the ratio of web crippling load P/P_{Exp}, and the vertical axis shows the ratio of moment M/M_{Exp}. The test strengths ($P_{\text{C-Exp}}$ and $M_{\text{C-Exp}}$) have been nondimensionalized with respect to the

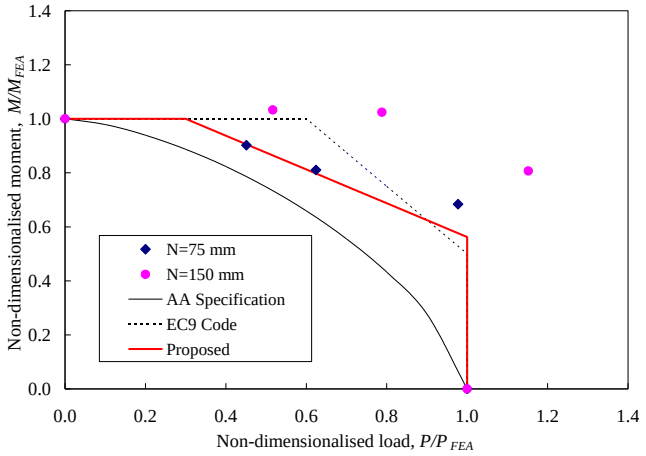

Fig. 9 Comparison of combined bending and web crippling numerical strengths with design strengths for square hollow section 150×150×1.7

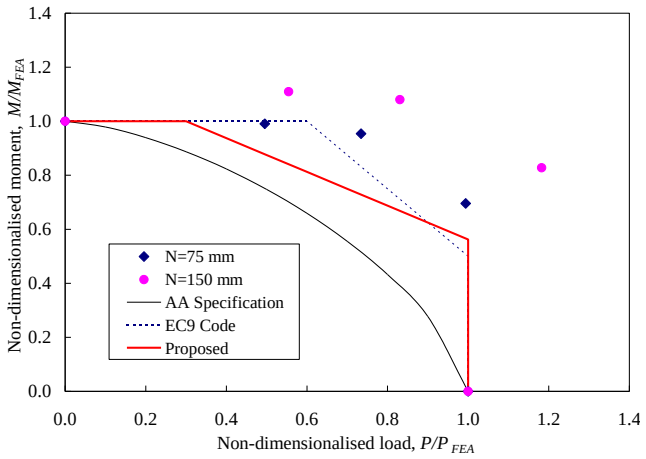

Fig. 10 Comparison of combined bending and web crippling numerical strengths with design strengths for square hollow section 150×150×2.5

experimental load per web (P_{Exp}) obtained from the pure web crippling tests and the experimental ultimate moment of the sections (M_{Exp}) obtained from the pure bending tests. Therefore, $P_{C\text{-}Exp}/P_{Exp}$ and $M_{C\text{-}Exp}/M_{Exp}$ were plotted for the combined bending and web crippling test strengths. It was shown that the design strengths predicted by the AA Specification are quite conservative for all specimens, as shown in Figs. 5-20. For EC9 Code, the design strengths are unconservative for aluminum specimens with small bearing lengths and large interaction factors (C-76×76×3N30K2.0, C-150×150×1.7N75K1.3, C-150×150×1.7N75K1.3, C-150×150×1.7N75K2.0, C-150×150×2.5N75K2.0, C-150×150×4.5N75K2.0, C-150×150×12.0N75K2.0, C-200×200×2.0N100K1.3, C-200×200×2.0N100K2.0, C-200×200×2.0N200K2.0, C-200×200×3.0N100K2.0 and C-200×200×25.0N100K2.0).

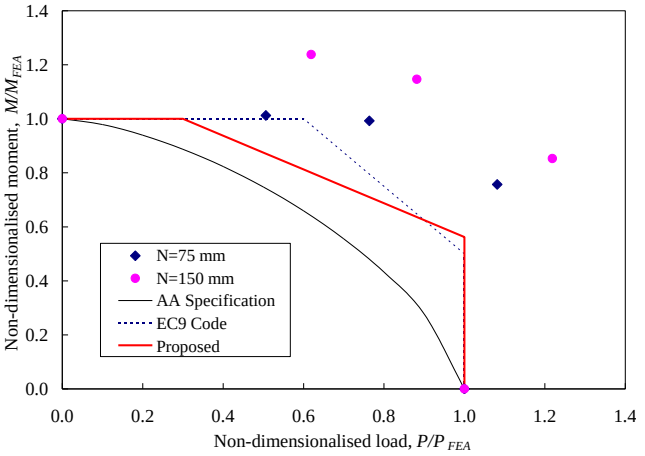

Fig. 11 Comparison of combined bending and web crippling numerical strengths with design strengths for square hollow section 150×150×3.0

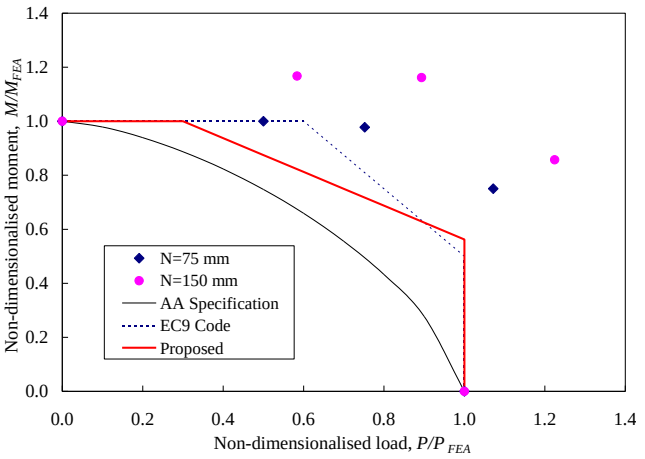

Fig. 12 Comparison of combined bending and web crippling numerical strengths with design strengths for square hollow section 150×150×3.5

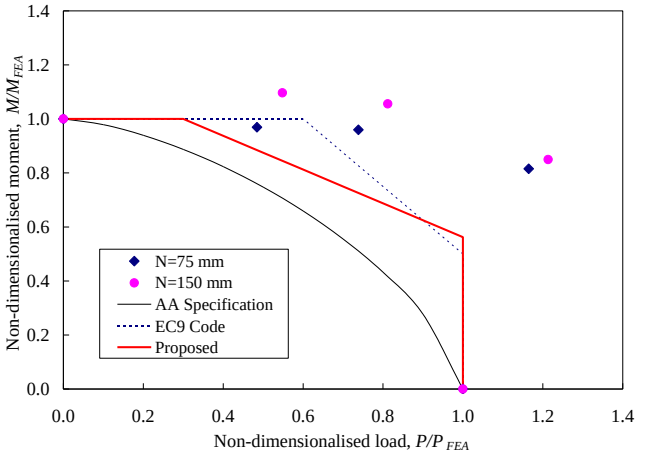

Fig. 13 Comparison of combined bending and web crippling numerical strengths with design strengths for square hollow section 150×150×4.5

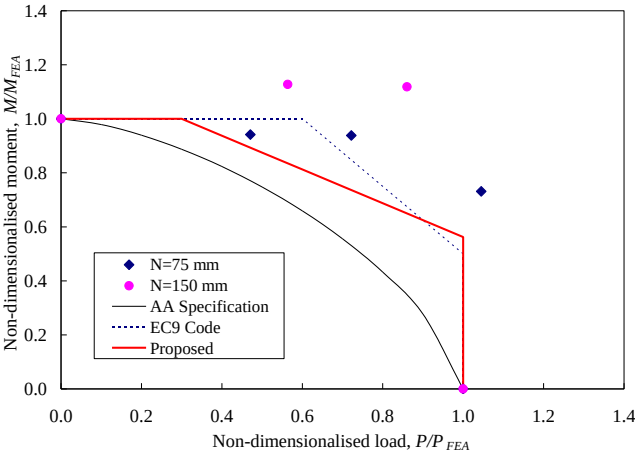

Fig. 14 Comparison of combined bending and web crippling numerical strengths with design strengths for square hollow section 150×150×12.0

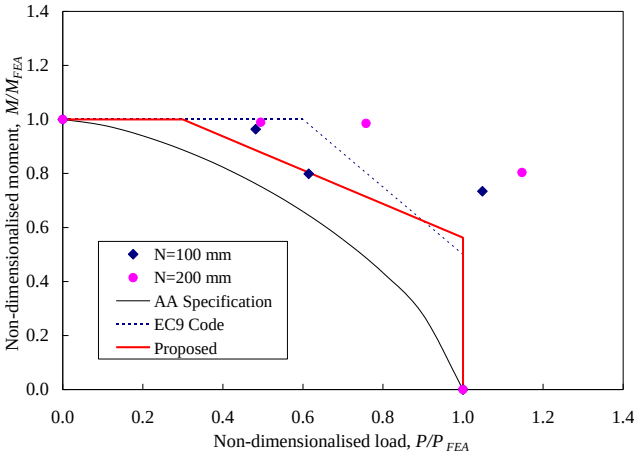

Fig. 15 Comparison of combined bending and web crippling numerical strengths with design strengths for square hollow section 200×200×2.0

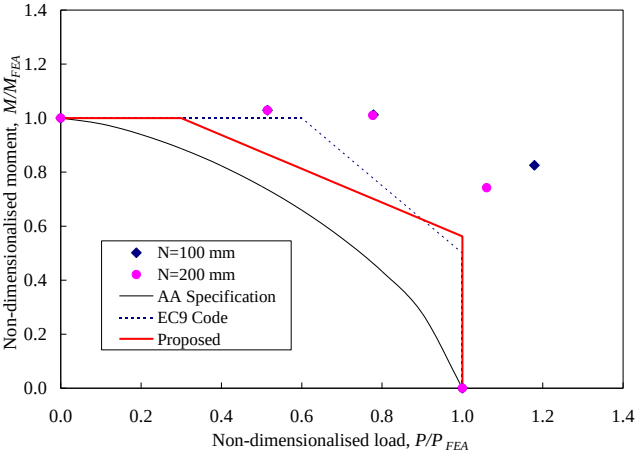

Fig. 16 Comparison of combined bending and web crippling numerical strengths with design strengths for square hollow section 200×200×2.5

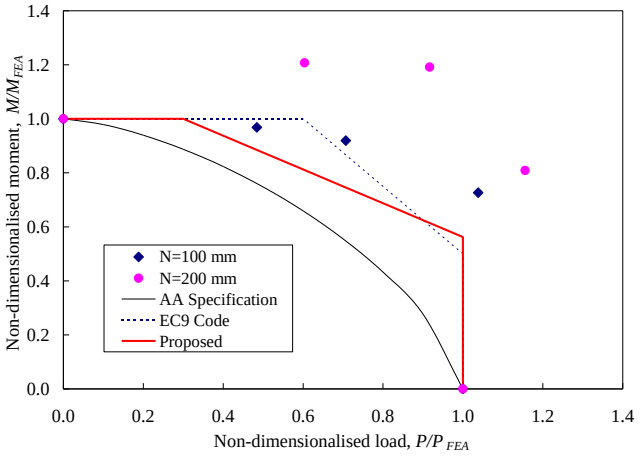

Fig. 17 Comparison of combined bending and web crippling numerical strengths with design strengths for square hollow section 200×200×3.0

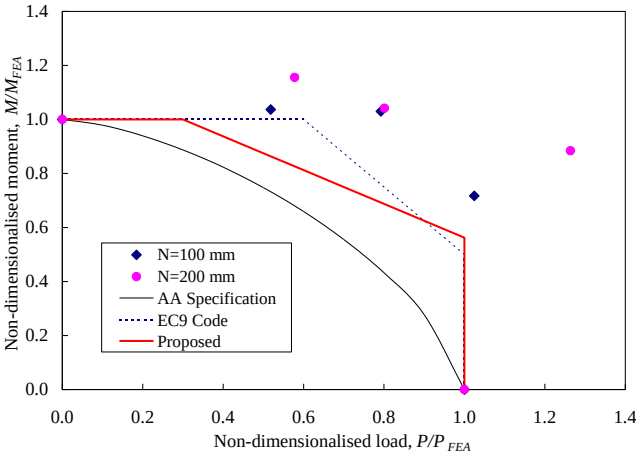

Fig. 18 Comparison of combined bending and web crippling numerical strengths with design strengths for square hollow section 200×200×5.5

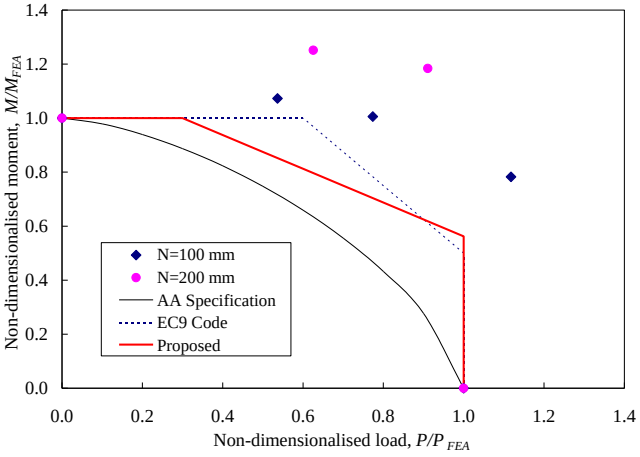

Fig. 19 Comparison of combined bending and web crippling numerical strengths with design strengths for square hollow section 200×200×9.0

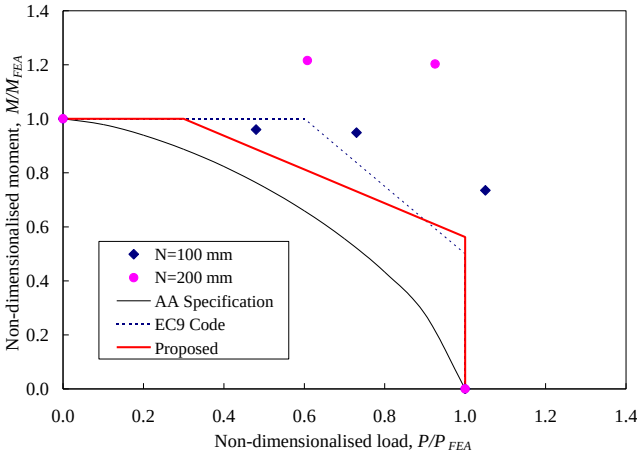

Fig. 20 Comparison of combined bending and web crippling numerical strengths with design strengths for square hollow section 200×200×25.0

7. Proposed design strengths and comparison with experimental and numerical results

The nominal strengths calculated using the AA Specification (2015), AS/NZS Standard (1997) and EC9 Code (2007) are either quite conservative or unconservative for aluminum square hollow sections subjected to combined bending and web crippling, as shown in Figs. 5-20. Hence, a bending and web crippling interaction equation for aluminum square hollow section specimens is proposed in this paper. The proposed design equation is as follows

$$\left(\frac{P}{P_{Exp}}\right)+1.6\left(\frac{M}{M_{Exp}}\right)\leq 1.9 \tag{4}$$

where P is the required web crippling strength per web, P_{Exp} is the experimental web crippling load per web obtained from the pure web crippling tests, M is the required flexural strength of the sections and M_{Exp} is the experimental ultimate moment of the sections obtained from the pure bending tests.

The experimental results obtained from the combined bending and web crippling tests and numerical strengths predicted from the finite element analysis are compared with the nominal strengths (unfactored design strengths) predicted using the proposed design equation. The proposed design strengths were calculated using the measured cross-section dimensions and measured material properties. The proposed design strengths are conservative for all the specimens and, especially, agree well with the experimental and numerical results for aluminum specimens with small bearing lengths and large interaction factors, as shown in Fig. 5-20.

8. Conclusions

Experimental and numerical investigations of aluminum tubular members subjected to combined bending and web crippling have been presented in this paper. A series of tests was performed to examine the appropriateness of the bending and web crippling interaction equation for aluminum square hollow sections in the current American Specification, Australian/New Zealand Standard and European Code for aluminum structures. The test specimens were extruded from heat-treated aluminum alloy of 6061-T6. The specimens were tested at various lengths to obtain the interaction relationship between bending moment and concentrated load. Finite element models including geometric and material non-linearities have been developed and verified against the experimental results obtained from this study and test data from existing literature for the pure bending tests, pure web crippling tests, and combined bending and web crippling tests. The finite element models closely predicted the behaviour of aluminum square hollow sections subjected to pure bending, pure web crippling and combined bending and web crippling compared with the test results. Hence, a parametric study was carried out to study the effect of cross-section geometries on the combined bending and web crippling strengths of aluminum square hollow sections.

The test results and the strengths predicted from the finite element analysis were compared with the design predictions obtained using the American Specification, Australian/New Zealand Standard and European Code for aluminum structures. It has been shown that the combined bending and web crippling design strengths predicted by the current specifications are either quite conservative or unconservative for aluminum square hollow sections. Therefore, a combined bending and web crippling design equation for aluminum square hollow section specimens is proposed in this study.

References

AA (2015), Aluminum design manual; The Aluminum Association, Arlington, VA, USA.

ABAQUS (2006), ABAQUS Standard User's Manual; Hibbitt, Karlsson and Sorensen, Inc., Vols. 1-3, Version 6.6, USA.

AS (1991), Methods for tensile testing of metals; Australian Standard AS 1391, Standards Association of Australia, Sydney, Australia.

AS/NZS (1997), Aluminium structures – Part 1: Limit state design; Australian/New Zealand Standard AS/NZS 1664.1: 1997, Standards Australia, Sydney, Australia.

ASTM (1997), Standard test methods for tension testing of metallic materials; E 8M-97, American Society for Testing and Materials, West Conshohocken, PA, USA.

AS4100 (1998), Steel Structures; AS 4100:1998, Standards Australia, Sydney, Australia.

BS5950 (2000), Structural use of Steelwork in Building. BS 5950, Part 1; British Standard Institution, London, UK.

Castaldo, P., Nastri, E. and Piluso, V. (2017a), "FEM simulations and rotation capacity evaluation for RHS temper T4 aluminium alloy beams", *Composites Part B*, **115**, 124-137.

Castaldo, P., Nastri, E. and Piluso, V. (2017b), "Ultimate behaviour of RHS temper T6 aluminium alloy beams subjected to non-uniform bending: Parametric analysis", *Thin-Wall. Struct.*, **115**, 129-141.

Chen, Y., Chen, X. and Wang, C. (2015), "Aluminum tubular sections subjected to web crippling", *Thin-Wall. Struct.*, **90**, 49-60.

De Matteis, G., Moen, L.A., Langseth, M., Landolfo, R.,

Hopperstad, O.S. and Mazzolani, F.M. (2001), "Cross-sectional classification for aluminum beams - parametric study", *J. Struct. Eng., ASCE*, **127**(3), 271-279.
EC9 (2007), Eurocode 9: Design of aluminum structures – Part 1.1: General structural rules; BS EN 1999-1-1:2007, European Committee for Standardization.
Gardner, L. and Nethercot, D. (2004), "Numerical modeling of stainless steel structural components-A consistent approach", *J. Struct. Eng., ASCE*, **130**(10), 1586-1601.
Jáger, B., Dunai, L. and Kövesdi, B. (2015), "Girders with trapezoidally corrugated webs subjected by combination of bending, shear and path loading", *Thin-Wall. Struct.*, **96**, 227-239.
Kövesdi, B., Alcaine, J., Dunai, L., Mirambell, E., Braun, B. and Kuhlmann, U. (2014), "Interaction behaviour of steel I-girders Part I: Longitudinally unstiffened girders", *J. Constr. Steel Res.*, **103**, 327-343.
Islam, S.M.Z. and Young, B. (2018), "Design of CFRP-strengthened aluminum alloy tubular sections subjected to web crippling", *Thin-Wall. Struct.*, **124**, 605-621.
Mazzolani, F.M. (1995), *Aluminum Alloy Structures*, (2nd Edition), E & FN Spon, London, UK.
Moen, L.A., Hopperstad, O.S. and Langseth, M. (1999a), "Rotational capacity of aluminum beams under moment gradient. I: Experiments", *J. Struct. Eng., ASCE*, **125**(8), 910-920.
Moen, L.A., De Matteis, G., Hopperstad, O.S., Langseth, M., Landolfo, R. and Mazzolani, F.M. (1999b), "Rotational capacity of aluminum beams under moment gradient. II: Numerical simulations", *J. Struct. Eng., ASCE*, **125**(8), 921-929.
Piluso, V., Pisapia, A., Nastri, E. and Montuori, R. (2019), "Ultimate resistance and rotation capacity of low yielding high hardening aluminium alloy beams under non-uniform bending", *Thin-Wall. Struct.*, **135**, 123-136.
Su, M. and Young, B. (2018), "Design of aluminum alloy stocky hollow sections subjected to concentrated transverse loads", *Thin-Wall. Struct.*, **124**, 546-557.
Sundararajah, L., Mahendran, M. and Keerthan, P. (2017), "Web crippling experiments of high strength lipped channel beams under one-flange loading", *J. Constr. Steel Res.*, **138**, 851-866.
Tryland, B.T., Langseth, M. and Hopperstad, O.S. (1999), "Nonperfect aluminum beams subjected to concentrated loading", *J. Struct. Eng., ASCE*, **125**(8), 900-909.
Vigh, L.G. (2012), "Influence of curved flange-to-web connection on the transverse load resistance of extruded or hot-rolled I girder", *Thin-Wall. Struct.*, **60**, 127-136.
Wu, C., Zhao, X.L., Duan, W.H. and Phipat, P. (2012), "Improved end bearing capacities of sharp-corner aluminum tubular sections with CFRP strengthening", *Int. J. Struct. Stabil. Dyn.*, **12**(1), 109-130.
Yu, W.W. (2000), *Cold-Formed Steel Design*, (3rd Edition), John Wiley and Sons, Inc., New York, NY, USA.
Zhao, X.L. and Hancock, G.J. (1992), "Square and rectangular hollow sections subject to combined actions", *J. Struct. Eng., ASCE*, **118**(3), 648-668.
Zhou, F. and Young, B. (2007), "Experimental and numerical investigations of cold-formed stainless steel tubular sections subjected to concentrated bearing load", *J. Constr. Steel Res.*, **63**(11), 1452-1466.
Zhou, F. and Young, B. (2008), "Aluminum tubular sections subjected to web crippling – Part I: Tests and finite element analysis", *Thin-Wall. Struct.*, **46**(4), 339-351.
Zhou, F. and Young, B. (2010), "Web Crippling of Aluminum Tubes with Perforated Webs", *Eng. Struct.*, **32**(5), 1397-1410.
Zhou, F., Young, B. and Zhao, X.L. (2009), "Tests and Design of Aluminum Tubular Sections Subjected to Concentrated Bearing Load", *J. Struct. Eng., ASCE*, **135**(7), 806-817.
Zhu, J.H. and Young, B. (2009), "Design of aluminum flexural members using direct strength method", *J. Struct. Eng., ASCE*, **135**(5), 558-566.

BU